BALLISTIC CASCADING AS A FORMATION MECHANISM FOR LUNAR COLD SPOT CRATERS: CONSTRAINTS ON THE IMPACT PROCESS FROM DIVINER THERMAL MEASUREMENTS.

C. E. Watkins[1], P. O. Hayne[2], J. L. Bandfield[3], and the Diviner Lunar Radiometer Science Team [1]St. Olaf College (watkinsc@stolaf.edu), [2]Jet Propulsion Laboratory, California Institute of Technology (Paul.O.Hayne@jpl.nasa.gov), [3]Space Science Institute.

Introduction Cold spots are a class of fresh impact craters recently revealed by their unusual thermal signatures in Diviner Lunar Radiometer data [1, 2, 3]. Though the details of their origins remain unknown, the near-crater deposits can be explained by a laterally propagating granular flow created by impact in the lunar vacuum environment [3]. Further from the source crater, at distances of 10–100 crater radii, regolith surfaces appear to have been "fluffed-up" without the accumulation of significant ejecta material. Our hypothesis is that these features form by a ballistic collisional cascade of ejecta particles. We utilized Diviner nighttime temperature data to derive near-surface thermal inertia profiles that can be used to characterize the physical properties of the regolith within the cold spots and test the formation hypothesis.

Characterization of Observed Cold Spots: Nighttime regolith cooling data from Diviner can be accurately fit [4] with exponential depth profiles of both conductivity and density, ρ, with the form:

$$\rho(z) = \rho_0 - \left(\rho_0 - \rho_s\right)^{-z/H} \quad ,$$

where ρ_s and ρ_0 are the density at the surface and at depth $z \gg H$, respectively. The parameter H has units of length, and characterizes the thickness of extremely low thermal inertia regolith in the upper ~10 cm [5]. Larger H-values indicate a lower density regolith.

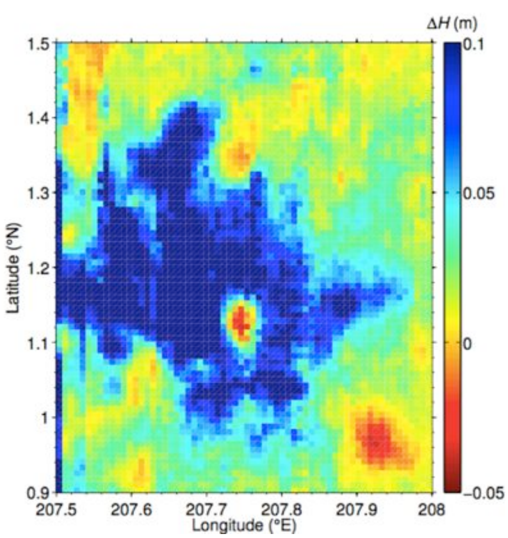

Figure 1: Example map of the upper regolith thickness parameter H.

From the extensive Diviner dataset, we generated 128 pixel-per-degree maps of H, and collected radial profiles of this parameter (Fig. 1). We were particularly interested in whether or not the cold spot radial profiles follow a consistent power law, which could be used to constrain formation models. For example, if the cold spots represent emplaced ejecta material, the thickness $H(r)$ might follow a similar distribution to the canonical power law relation for ejecta thickness,

$$t(r) = t_0 \left(r/R_c\right)^{-\beta}$$

where r is distance from the crater rim (radius R_c), and β (≈ 3) is derived from lunar crater data [6].

We selected 10 equatorial cold spot craters of similar size where observational artifacts from slope features have the least effect on the H-parameter calculation from Diviner thermal data. Figure 1 shows an equatorial cold spot map of ΔH, which is the difference from typical lunar surfaces. The pattern of a small warmer (negative ΔH-value) region surrounding the crater is indicative of the effects of small rocks and debris, which offset the H-parameter calculations of thermal inertia. This near-crater rocky region of regolith limited the search for power law attributes of the H-parameter to a more distal ~10 to ~50 crater radii, as farther than ~50 crater radii the cold spot signature dropped off precipitously. Each of the cold spot ΔH maps was fitted with a basic power law equation, $\Delta H(r) = A(r/R_c)^{-B}$. In the regions of interest for each cold spot, we found that the thickness parameter fol-

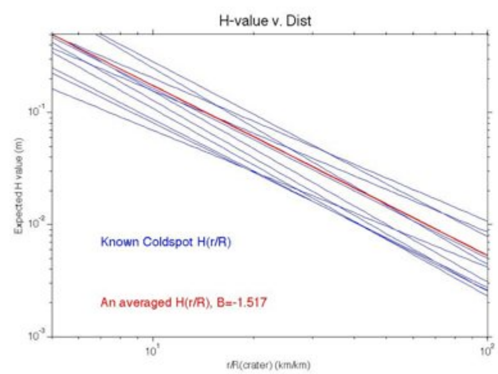

Figure 2: Log-log plot of ΔH vs. distance from crater rim for 10 equatorial cold spots (blue lines), along with the average power law fit of ~3/2 (red line)

lows the power law $H \sim (r/R_c)^{-3/2}$. In fact, the results indicate a consistent value of B ($B = 3/2 \pm 0.2$), and a larger variance in A (Figure 2). The variance in the A term is not directly linked to crater size. We used ultraviolet “optical maturity” [7] to check whether this parameter correlates with relative crater age, but again did not observe a strong trend.

Modeling: Energy balance provides a way of testing cold spot formation models, given the derived radial density profile power law $B \sim 3/2$. We calculated a detailed energy budget for the cold spot shown in Fig. 1, with expected kinetic energy input K compared to the potential energy ΔU required to change the density profile as manifested in ΔH:

$$\Delta U / g = (\rho_0 - \rho_s)(d'H' - d_0 H_0) + \frac{\rho_0}{2}(d_0^2 - d'^2)$$

$$K / g \approx \frac{\rho_s}{2} t(r) r$$

where H_0 is the background H-parameter value, d_0 is the initial depth of the column, and the new depth is given by

$$d' = d_0 + \frac{\rho_0 - \rho_s}{\rho_0} \Delta H$$

We make three basic assumptions: 1) the total change in the effective density profile occurs within the top meter of soil, 2) for the density profile $\rho_s = 1000$ kg/m^3 and $\rho_o = 1800$ kg/m^3, and 3) the background H-parameter is 7 cm.

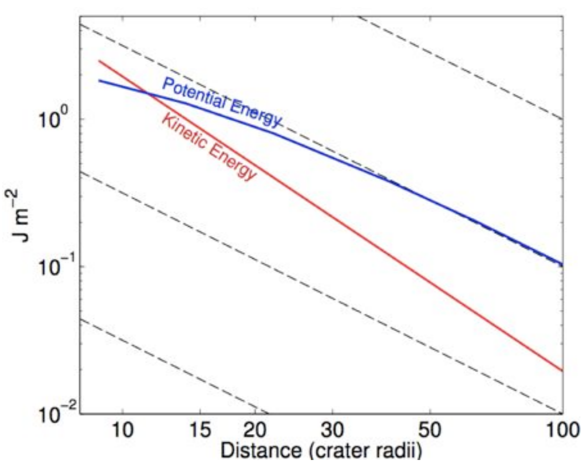

Figure 3: Log-log plot of available kinetic energy from ballistic ejecta particles, and change in potential energy due to regolith decompression for the cold spot in Fig. 1.

Fig. 3 shows the dominance of kinetic energy deposition close to the crater and a defict beyond ~10 R_c. The imbalance of imparted kinetic energy and potential energy change provides insight about the possible cold spot formation mechanisms. The excess change in potential energy must come from a redistribution of the thermal and kinetic energy of the impactor. In order to test the possibility of a collisional cascade pushing the kinetic energy radially outward in order to made up for the discrepancy of potential energy, we developed a soft sphere discrete element model (SSDEM). The model follows the methodology of Kruggel-Emden [8], tracking particles to understand how ballistic impact velocity affects the directionality and energy of the tertiary ejecta particles.

From the experiments of Salisbury *et al.* [9], we can assert that particles reaching a maximum height < 10 cm will cause net decompression of the regolith. We ran an ensemble of models to test for the maximum height of a collision chain of 10,000 particles and performed a statistical analysis of the results. We also ran the SSDEM with variable secondary impact angles and velocities to understand the change in response from the regolith. The results suggest that as particles travel further, the tertiary ejecta become radially? symmetrical. The power law for $\Delta H(r)$ derived strictly from the SSDEM maximum height resulted in a power of $\beta \sim 1.2$ versus the actual 1.5 from the Diviner data. This similarity suggests ballstic cascading remains a viable explanation for the cold spots, though a more complete dynamical model including thermal dissipation and melting could yield more accurate results.

Conclusions: Data from Diviner show that lunar cold spots display a remarkably consistent power law behavior in their radial regolith density profiles, with $\log H(r) \sim -3/2$. This consistency argues for a common formation mechanism. Our preliminary results suggest ballistic cascading is a plausible formation mechanism for cold spots. The SSDEM methodology presents a novel way of investigating impact cratering through the complex process of particle collisional cascading. The effect yields a behavior which could account for the “pushbrooming” of fluffed regolith in distal regions.

References: [1] Paige D. A. et al. (2010), *Space Sci. Rev.*, *150*, 125, [2] Bandfield J. L. et al. (2014) *Icarus*, 10.1016/j.icarus.2013.12.017, [3] Bandfield J. L. et al. (2011) *J. Geophys. Res.*, 10.1029/2011JE003866, 2011. [4] Vasavada et al., 2012, [5] Hayne, P. O. (2013). *BAAS* 45, #9, 107.3, [6] McGetchin T. R. et al. (1973) *Earth and Planet. Sci. Lett.*, *20*, 226-236, [7] Lucey P. G. et al. (2000), *J. Geophys. Res.*, *105*, [8] Kruggel-Emden H. et al. (2007) *Powder Technology*, *171*, 157-173, [9] Salisbury J. W. and J. E. M. Adler (1967), *Nature*, *214*, 156-158.